

AD-A196 531

Plastic Flow
in
Oriented Glassy Polymers

by
Mary C. Boyce, David M. Parks, Ali S. Argon

Massachusetts Institute of Technology

October, 1987

4
S DTIC
ELECTE
JUN 03 1988
D

Abstract

A manufactured product often possesses residual texture which was either incidentally or deliberately acquired during its processing history. This is particularly true for the case of polymers, where the ability to easily preferentially pre-orient the material in specific directions is exploited in order to obtain a higher strength product. Specific examples include synthetic fibers, and biaxially-oriented films and containers. The response of the pre-oriented/textured product to normal service life loading conditions will differ considerably from that of a product composed of isotropic material. This paper addresses the issue of the effects of texture on the deformation behavior of glassy polymers. Here, the physically-based constitutive model of Boyce, Parks, and Argon [1987] describing the rate, temperature, and pressure dependent inelastic deformation of initially isotropic glassy polymers is extended to include effects of pre-orientation, i.e. initial texture, via the use of appropriate initial conditions on internal state variables. The modified model is then utilized in an analysis of the effects of texture on the yield of glassy polymers and the shear localization which normally follows yielding in oriented polymers. These results are compared with trends found in experiments as reported in the literature. The effectiveness of the proposed model for the present application is also compared with earlier models of yielding of anisotropic materials such as Hill's criterion.

DISTRIBUTION STATEMENT A

Approved for public release;
Distribution Unlimited

REPORT DOCUMENTATION PAGE

1a REPORT SECURITY CLASSIFICATION UNCLASSIFIED		1b RESTRICTIVE MARKINGS NONE			
2a SECURITY CLASSIFICATION AUTHORITY		3 DISTRIBUTION AVAILABILITY OF REPORT Approved for public release. Distribution unlimited.			
4b DECLASSIFICATION DOWNGRADING SCHEDULE					
4 PERFORMING ORGANIZATION REPORT NUMBER(S) Technical Report No. 2		5 MONITORING ORGANIZATION REPORT NUMBER(S)			
6a NAME OF PERFORMING ORGANIZATION Massachusetts Institute of Technology	6b OFFICE SYMBOL (If applicable)	7a NAME OF MONITORING ORGANIZATION ONR			
6c ADDRESS (City, State, and ZIP Code) 77 Massachusetts Avenue Cambridge, MA 02139		7b ADDRESS (City, State, and ZIP Code) 800 North Quincy Street Arlington, VA 22217			
8a NAME OF FUNDING/SPONSORING ORGANIZATION DARPA	8b OFFICE SYMBOL (If applicable)	9 PROCUREMENT INSTRUMENT IDENTIFICATION NUMBER N00014-86-K-0768			
8c ADDRESS (City, State, and ZIP Code) 1400 Wilson Boulevard Arlington, VA 22209		10 SOURCE OF FUNDING NUMBERS			
		PROGRAM ELEMENT NO.	PROJECT NO	TASK NO	WORK UNIT ACCESSION NO.
		R & T Code	A400005		
11 TITLE (Include Security Classification) PLASTIC FLOW IN ORIENTED GLASSY POLYMERS					
12 PERSONAL AUTHOR(S) Boyce, Mary C.; Parks, David M., and Argon, Ali S.					
13a. TYPE OF REPORT Journal paper	13b. TIME COVERED FROM 1/15/87 TO 6/30/88		14. DATE OF REPORT (Year, Month, Day) 1987, October	15 PAGE COUNT 43	
16. SUPPLEMENTARY NOTATION Submitted for publication in International J. Plasticity.					
17 COSATI CODES		18 SUBJECT TERMS (Continue on reverse if necessary and identify by block number) Plastic flow; glassy polymers, texture, oriented polymers, computer simulation of plastic flow. <i>SEC</i>			
19 ABSTRACT (Continue on reverse if necessary and identify by block number) A manufactured product often possesses residual texture which was either incidentally or deliberately acquired during its processing history. This is particularly true for the case of polymers, where the ability to easily preferentially pre-orient the material in specific directions is exploited in order to obtain a higher strength product. Specific examples include synthetic fibers, and biaxially-oriented films and containers. The response of the pre-oriented/textured product to normal service life loading conditions will differ considerably from that of a product composed of isotropic material. This paper addresses the issue of the effects of texture on the deformation behavior of glassy polymers. Here, the physically-based constitutive model of Boyce, Parks, and Argon [1987] describing the rate, temperature, and pressure dependent inelastic deformation of initially isotropic glassy polymers is extended to include effects of pre-orientation, i.e., initial texture, via the use of appropriate initial conditions on internal state variables. (Continues on reverse side)					
20 DISTRIBUTION/AVAILABILITY OF ABSTRACT <input checked="" type="checkbox"/> UNCLASSIFIED/UNLIMITED <input type="checkbox"/> SAME AS RPT <input type="checkbox"/> DTIC USERS			21 ABSTRACT SECURITY CLASSIFICATION Unclassified		
22a NAME OF RESPONSIBLE INDIVIDUAL A.S. Argon			22b TELEPHONE (Include Area Code) (617) 253-2217		22c. OFFICE SYMBOL

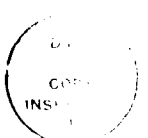
19. Abstract (Continuation)

The modified model is then utilized in an analysis of the effects of texture on the yield of glassy polymers and the shear localization which normally follows yielding in oriented polymers. These results are compared with trends found in experiments, as reported in the literature. The effectiveness of the proposed model for the present application is also compared with earlier models of yielding of anisotropic materials such as Hill's criterion.

1 Introduction

Texture affects both the elastic and the inelastic behavior of a polymer. However, the effect of texture on the inelastic response is far greater than that on the elastic response, especially for glassy polymers. Hadley [1975] has summarized the effect of orientation on the small strain elastic properties of polymers. He reports that, whereas the elastic tensile modulus of some semi-crystalline polymers may increase by more than an order of magnitude at large draw ratios, the largest increase in the modulus of amorphous polymers was found in PMMA and was only 30% (Wright, *et al.* [1971]). This increase in elastic modulus with orientation is very small and would have little impact on the material undergoing large inelastic deformation, where the effect of orientation on the yield strength of the material is considerable. Therefore, for the purposes of this work, orientation effects on the elastic response of the material will be neglected.

The effect of texture on the inelastic response of glassy polymers will now be examined. In order to best understand the oriented polymer, the primary physical mechanisms governing plastic flow in initially isotropic glassy polymers will first be reviewed. We will then present a three-dimensional constitutive model for initially isotropic glassy polymers proposed by Boyce, Parks, and Argon [1987a]. The presence of an initial texture on the basic macromolecular structure of the polymer and its impact on the deformation resistances will then be discussed. These observations will lead us to incorporate texture effects into the constitutive model *via* the use of initial conditions on internal state variables. Finally, the plastic flow in oriented glassy polymers will be quantitatively examined using the model in conjunction with the finite element method. In particular, the effects of texture on the initial yield and subsequent shear localization will be analyzed. The numerical results will be compared with behavior trends which have been observed experimentally and reported in the polymer literature.



By _____	
Distribution/	
Availability Codes	
Dist	Avail. < or Special
A-1	

2 Inelastic Deformation of Glassy Polymers

In general, the yield of initially isotropic glassy polymers has been found to depend on strain rate, pressure and temperature. After yielding, polymers often strain soften and subsequently strain harden. These characteristics of yielding in glassy polymers are considered to result from two physically distinct sources of internal resistance (Haward, Thackray [1968], Argon [1973], Ward [1984]). To best describe these mechanisms, we assume an idealized material structure consisting of a random array of long molecular chains which intersect one another, forming points of entanglement [Figure 1]. This results in an isotropic network-like structure much like that of rubber, but with the chemical crosslinks replaced by physical entanglements. This structure is now loaded. At yield, an isotropic intermolecular resistance to chain segment rotation must be exceeded; this is a thermally-activated process. Once the material is free to flow, molecular alignment occurs, resulting in an anisotropic internal resistance to further inelastic deformation. Below, we discuss these deformation resistances to chain segment rotation and subsequent molecular alignment.

2.1 Intermolecular Resistance

The intermolecular resistance to plastic flow is due to the impedance imposed by neighboring chains on the ability of a chain segment to rotate either individually or in a cluster. Argon [1973] has developed an expression for the plastic shear strain rate, $\dot{\gamma}^p$, which results once the free energy barrier to chain segment rotation in an equivalent isotropic elastic medium has been overcome:

$$\dot{\gamma}^p = \dot{\gamma}_0 \exp\left[-\frac{As_0}{\Theta}\left(1 - \left(\frac{\tau}{s_0}\right)^{\frac{1}{1-\nu}}\right)\right]; \quad (1)$$

where $\dot{\gamma}_0$ is the pre-exponential factor; A is proportional to the activation volume/Boltzmann's constant; Θ is the absolute temperature; $s_0 = \frac{0.077}{1-\nu}\mu$ is the athermal shear strength, μ is the elastic shear modulus, and ν is Poisson's ratio; τ is the applied shear stress. This expression has been extended by Boyce, *et al.* [1987a] to include the effects

of pressure and strain softening. In the modification, the athermal shear strength s_0 is replaced by $s + \alpha p$, where p is the pressure, α is the pressure dependence coefficient, and s is now taken to evolve with plastic straining. The initial condition on s is the annealed value s_0 . The shear resistance is phenomenologically modelled to decrease with plastic straining until reaching a "preferred" structure, represented by s_{ss} , via $\dot{s} = h(1 - \frac{s}{s_{ss}})\dot{\gamma}^p$, where h is the rate of resistance drop with respect to the plastic strain, and s_{ss} generally depends on Θ and $\dot{\gamma}^p$. The evolution of s with plastic strain models the macroscopic response of true strain softening. Softening is considered to be the result of local dilatation which accompanies micro-shear banding during plastic flow (Argon, *et al.* [1985]). Any fluctuations in local volume would obviously impact the intermolecular resistance. This leads to the phenomenological model of s given above. Thus, s is taken to be an internal state variable which monitors the isotropic resistance to deformation. The shear resistance is also known to increase with pressure, time, and temperature, *i.e.* the material physically ages (Kramer [1970], Struik [1978], Haward [1980]). Although aging is not currently included in the model, it is important to mention this phenomenon prior to the later discussion on initial conditions for internal state variables.

2.2 Network Resistance

Once the material is stressed to the point of overcoming intermolecular barriers to chain motion, the molecular chains will tend to align along the direction of principal plastic stretch. This action decreases the configurational entropy of the system which, in turn, creates an internal network stress state. Following mechanics terminology, we call this internal stress the back stress tensor, \mathbf{B} . Due to the rubbery network-like response of glassy polymers to plastic deformation (see (Boyce, *et al.* [1987a], Ward [1984])), the back stress has been modelled using a statistical mechanics of rubber elasticity model. We have assumed that the initial network structure of the polymer is isotropic. Subsequent network orientation is taken to coincide with plastic stretching, and \mathbf{B} is

taken to be coaxial with the plastic stretch. In terms of principal components, B may be expressed as:

$$\bar{B}_i = \bar{B}_i(\lambda_j^p / \lambda_L); \quad (2)$$

where \bar{B}_i is a principal component of the back stress tensor; λ_j^p are the principal network (and plastic) stretch components; λ_L is the locking network stretch or natural draw ratio of the material. The model is based on a Langevin spring formulation such that B_i becomes infinitely large as λ_j^p / λ_L approaches 1, and $B_i = 0$ for the isotropic case of $\lambda_j^p = 1$.

Above we gave a brief summary of the resistances to plastic flow in an essentially one-dimensional framework. These ideas have been incorporated into a fully three-dimensional representation of inelastic behavior which is summarized immediately below.

2.3 Three-Dimensional Representation

We first consider the deformation of an initially isotropic body, B_0 . The body is loaded to a state, B_t , and its deformed configuration may be described by the deformation gradient, \mathbf{F} , at this time. The deformation gradient may be multiplicatively decomposed into elastic and plastic components, $\mathbf{F} = \mathbf{F}^e \mathbf{F}^p$ (Lee [1969]). Here, with no loss of generality (Boyce, et al. [1987c]), we take \mathbf{F}^e to be symmetric, i.e. \mathbf{F}^p represents the relaxed configuration obtained by elastically unloading without rotation (in the polar decomposition sense) to a stress-free state. The rate quantities corresponding to this formulation consist of the velocity gradient:

$$\mathbf{L} = \dot{\mathbf{F}} \mathbf{F}^{-1} = \mathbf{D} + \mathbf{W} = \dot{\mathbf{F}}^e \mathbf{F}^{e-1} + \mathbf{F}^e \dot{\mathbf{F}}^p \mathbf{F}^{p-1} \mathbf{F}^{e-1}, \quad (3)$$

where \mathbf{D} is the rate of deformation, and \mathbf{W} is the spin. The velocity gradient of the relaxed configuration is given by $\mathbf{L}^p = \dot{\mathbf{F}}^p \mathbf{F}^{p-1} = \mathbf{D}^p + \mathbf{W}^p$. As discussed in Onat [1987], the spin of the relaxed configuration, \mathbf{W}^p , is algebraically defined as a result of the symmetry imposed on the elastic deformation gradient. The rate of shape change,

D^p , must be constitutively prescribed. The magnitude of D^p is given by the plastic shear strain rate, $\dot{\gamma}^p$, and the tensor direction of D^p is specified by $N = \frac{1}{\sqrt{3r}} T''$, the normalized deviatoric portion of the driving stress state, T'' , at a material point. This driving stress state, T'' , is given by the tensor:

$$T'' = T - \frac{1}{J} F'' B F'', \quad (4)$$

where: T is the Cauchy stress tensor; J is the volume change given by $\det F''$; and B is the back stress tensor due to strain hardening resulting from molecular alignment. We refer to T'' as the driving stress state because it is only this portion of the stress which continues to activate plastic flow. The back stress portion is an internal stress which acts as a resistance. The back stress tensor is taken to be an isotropic function of the left plastic stretch tensor:

$$F'' = V'' R''; \text{ polar decomposition} \quad (5)$$

$$V'' = \bar{R}''^T \bar{V}'' \bar{R}''; \text{ eigen value decomposition} \quad (6)$$

$$\bar{B}_i = \bar{B}_i (\bar{V}_j'' / \lambda_L). \quad (7)$$

The effective equivalent shear stress, τ , is given by:

$$\tau = [\frac{1}{2} T'' \cdot T'']^{\frac{1}{2}}. \quad (8)$$

The plastic shear strain rate, $\dot{\gamma}^p$, was constitutively prescribed in equation (1). However, τ is now taken to be the effective equivalent shear stress given above in equation (8).

2.4 Effect of Initial Texture on Micromechanisms of Flow

Now, we consider the effects of pre-orientation on the two resistances to plastic flow - intermolecular interaction and molecular alignment. The intermolecular resistance is a restriction on molecular motion due to surrounding chains. One could argue that this resistance may change with material orientation for a number of reasons. At very large deformations, after much molecular alignment has occurred, the volume fraction

of sites which have yet to overcome intermolecular barriers has greatly decreased. The presumably higher barriers of the remaining population would result in an isotropic hardening component which could be phenomenologically accounted for within the current framework of the model by an increasing athermal shear resistance s as very large deformations are reached. We also note that the intermolecular resistance is a function of the elastic shear modulus. In section one, we concluded that the effects of pre-orientation on the elastic properties are small and, in fact, negligible in the current context of application of this work. In order to accurately assess the effects of developing anisotropy of the elastic moduli on s , an equation for the plastic shear strain rate (equation (1)) would have to be derived considering chain segment rotation in an anisotropic elastic medium. This effect would become noticeable only at very large deformations, at which point, it would also be comparatively small with respect to the asymptotically increasing back stress. Therefore, in our modelling, the effects of pre-orientation on the intermolecular resistance will be neglected. On the other hand, the network resistance, *i.e.* the back stress tensor, is obviously greatly affected by the presence of an initial orientation, since it is a direct result of molecular alignment.

The above discussion leads us to model texture/orientation in glassy polymers as an initial network stretch in the material, which has a corresponding initial back stress. In other words, before plastic flow commences in a textured polymer, in addition to the intermolecular resistance, an initial back stress must also be overcome. Figure 2 depicts a schematic of the true stress-stretch curve of an initially isotropic glassy polymer which is loaded, unloaded, and then reloaded without allowing for aging to occur. The effect of the initial loading (which orients the material) upon the stress level at which subsequent plastic flow commences is apparent upon reloading, *i.e.*, elevated levels of "peak yield" stresses are observed in the direction of the principal orientation. It is an oriented state such as this that is now our starting point. Experiments by Ward [1984] on cold-rolled and spun PET and by Bahadur [1973] on cold-rolled PC greatly support this concept of principal orientation as a description of state in glassy polymers.

2.4.1 Incorporation of Initial Texture into Constitutive Model

We now consider the incorporation of an initial texture into the above constitutive model. Prior to doing so, it is important to recall the idea of monitoring and describing the "state" of any material by the use of internal variables. The concept of internal state variables has achieved growing acceptance in the plasticity field in recent years (Kocks, Argon, and Ashby [1975], Rice [1975], Onat [1982], Nemat-Nasser [1983], Loret [1983], Dafalias [1985], Anand [1985]). In principle, an adequate number of internal variables will uniquely describe the current state of a material without regard to prior history of loading. Therefore, if given the instantaneous values of the relevant internal state variables in a given material, one should, using suitable evolution equations, be able to accurately predict the material response with no other knowledge of the process or history by which this state was achieved.

In this work, we are putting the concept of the internal state variable to full use. In the model for the initially isotropic glassy polymer, it was proposed that the current state of the material may be described by the stress tensor, T , the absolute temperature, Θ , the athermal shear resistance, s , and the back stress tensor, B . Furthermore, the back stress tensor is taken to be a state function of the plastic stretch measured with respect to the configuration possessing an isotropic network. More fundamentally, this portion of state description is described by a *network* stretch tensor, relative to an initial isotropic network configuration. The coincidence of the "plastic" and "network" stretches follows from the affine connection between molecular alignment and deformation. For the case of the oriented glassy polymer, we propose that the constitutive model for the initially isotropic glassy polymer also properly models the behavior of the corresponding oriented material when appropriate initial conditions are used on the athermal shear resistance, s , the network stretches, which will be called Δ^i , and, of course, if any residual stresses exist, the stress tensor, T . In turn, the initial value of the back stress tensor B will be taken as a function of (cf. equations 5-7) of Δ^i . Below, we will not consider residual stresses, but this would not significantly alter the basic

framework of modifications to be presented.

In order to best describe the incorporation of preorientation into the model by the use of initial conditions on the internal variables s and \mathbf{A}^i , we will consider the deformation of two bodies — the initially isotropic body and the initially oriented body. The deforming bodies are schematically illustrated in Figures 3(a) and (b), which also depict the initial conditions and the deformation of the underlying macromolecular network structure. The various loaded and relaxed configurations are described by their appropriate deformation gradients in the diagram. For the case of the initially isotropic body, the initial texture of the undeformed body, B_0 , may be described by the identity tensor, \mathbf{I} , indicating no preferred texture in the body. This is further illustrated by the initially isotropic network structure shown in Figure 3(a). In other words, in the model of Boyce, *et al.*, the initial network stretch was implicitly assumed to be identity. Earlier, we mentioned that the initial condition on the athermal shear resistance for the material in the annealed state is given by $s_0 = \frac{0.0774}{1-\nu}$. The deformation and consequent kinematic representation of the initially isotropic body was discussed earlier.

For the corresponding case of the initially oriented body, the initial texture of the body, B_0 , may now be described by the tensor \mathbf{A}^i , which describes the network preorientation of the body in terms of initial stretch ratios. This is also further illustrated by the initially oriented or stretched network structure shown in Figure 3(b). We wish to emphasize here that *this initial texture was not necessarily achieved by plastic working of the material*, but could have been otherwise obtained, *e.g.*, by a spinning process. The body is now deformed via \mathbf{F} , where \mathbf{F} describes the applied deformation gradient relative to the preoriented state. Returning to the initially textured relaxed configuration in Figure 3b, we note that one could imagine the existence of a "pre-reference" configuration possessing an isotropic network, such that both the state and shape of the textured reference configuration B_0 could, in principle, have been obtained by applying the (plastic and network) stretch \mathbf{A}^i to the pre-reference state and configuration. The deformation of a material element relative to this hypothetical con-

figuration may be described by $\mathbf{F}\Delta^i$. When the body is elastically unloaded without rotation, the relaxed configuration, relative to the preoriented state, is given by \mathbf{F}^p . However, the deformation of the relaxed configuration with respect to our hypothetical pre-reference configuration possessing an isotropic network structure, would be given by $\mathbf{F}^p\Delta^i$. Therefore, the initial texture given by the initial network stretch, Δ^i , may be operationally interpreted as an initial plastic stretch tensor (for modelling purposes). *The initial condition of texture is incorporated into the model as an initial plastic deformation gradient.* Such an initial condition is obtainable in a glassy polymer by reduction of birefringence data (Kahar, *et al.* [1978], Ward [1984], Botto, *et al.* [1984]). In the initially isotropic polymer, the back stress tensor was taken to be coaxial with the left plastic stretch tensor because the latter coincided with the network stretch. In the current sense, the network stretch and the resulting back stress is a result of texturing which occurred both prior to and directly from the currently applied deformation. Explicitly, we take the back stress tensor to be coaxial with the left stretch tensor of the product $\mathbf{F}^p\Delta^i$. We will call this product the network deformation gradient, \mathbf{F}^N . The back stress would be obtained as follows:

$$\mathbf{F}^N = \mathbf{F}^p\Delta^i, \quad (9)$$

$$\mathbf{F}^N = \mathbf{V}^N \mathbf{R}^N, \text{ polar decomposition} \quad (10)$$

$$\mathbf{V}^N = \bar{\mathbf{R}}^{NT} \bar{\mathbf{V}}^N \bar{\mathbf{R}}^N, \text{ eigen value decomposition} \quad (11)$$

$$\bar{B}_i = \bar{B}_i(\bar{V}_j^N / \lambda_L). \quad (12)$$

Note that the locking network stretch, λ_L , is that of the isotropic network structure.

The initial value for the athermal shear resistance in the textured polymer must be determined. In general, the method of preorientation is unknown. Thus, the occurrence of strain-softening and/or subsequent physical aging is also unknown. Therefore, currently, the initial value for s is obtainable by conducting a stress-strain test and observing if strain-softening occurs.

In the incorporation of preorientation into the equations of the constitutive model given earlier, there are three major items to recall. First, the deformation gradient F is with respect to the initial oriented state. Second, the back stress tensor results from all contributions to molecular alignment, past and present. In other words, the back stress tensor is measured with respect to the pre-reference isotropic state of the network. Since this is a major contribution to the plastic flow resistance, it is very important to get a good measurement of the initial orientation, Λ^i . The third item is the initial value of the athermal shear resistance, which may or may not be that of the annealed state. Therefore, the constitutive model is then numerically integrated and incorporated into the ABAQUS [1984] finite element code as done in Boyce, et al. [1987b], where an initial condition on the plastic deformation gradient of Λ^i is now included.

3 Effects of Preorientation on Material Behavior

Below, we will quantitatively examine the effects of texture on the plastic flow of a polymer. During homogeneous deformation, the stress at which active plastic flow begins is affected by both the degree and the orientation of the initial texture. Simulated tensile tests will be used to investigate this response. Polymers are also known to exhibit "shear banding", highly localized regions of straining, during plastic flow. Experiments (e.g., Brown and Ward [1968], Duckett [1975], Rider and Hargreaves [1969]) have shown that the direction of shear banding in polymers is also affected by both the amount of texture present in the material and its orientation with respect to the principal direction of loading. This behavior is also examined with our constitutive model and simulated tensile tests. The numerical results are compared with behavior trends reported in the literature.

3.1 "Homogeneous" Behavior

The effect of orientation on the initial flow behavior of a glassy polymer is now examined. We first consider some experimental results from tensile tests on oriented polymers. Secondly, we discuss an anisotropic yield criterion which has been applied to such polymers in the past. Finally, using the constitutive model given earlier, we analyze plastic flow in an oriented glassy polymer.

3.1.1 Previous Work

Tensile tests on thin specimens of oriented polymers have been conducted by Rider and Hargreaves [1969, 1970] on amorphous polyvinyl chloride (PVC), by Brown, *et al.* [1968a, b] on semi-crystalline (nearly amorphous) polyethylene terephthalate (PET), and by Duckett, *et al.* [1972] on semi-crystalline polypropylene (PP). These investigators have taken the initial texture of these test specimens to be described by the principal stretches: $\lambda_1 = \lambda$, $\lambda_2 = \lambda_3 = 1/\sqrt{\lambda}$, where λ is called the initial draw ratio (IDR). The orientation of the texture of a specimen when tested in simple tension is given by its initial draw direction (IDD) which is the angle, θ , that the first principal stretch makes with the tensile axis (Figure 4). Results of the yield stress¹ of the above materials with given IDRs as a function of IDD when tested in tension (at a fixed displacement rate) are shown in Figure 5. These materials exhibit a significant drop in the peak stress as the IDD deviates from the tensile axis, followed by a gradual levelling off of this stress at an IDD of approximately $\theta \approx 60^\circ$. Brown, *et al.* and Rider and Hargreaves then determined, from their experimental data, the coefficients for an anisotropic yield criterion.

A criterion for yield in materials which have been preferentially oriented, *e.g.* by deformation processing, such that they retain three mutually orthogonal planes of sym-

¹ Here, we use the term yield stress to describe either i) the peak stress before softening, if softening occurs; or, ii) the stress at the point where the tangents to the elastic and hardening portions of stress-strain curve intersect.

metry, has been proposed by Hill [1950]. The yield surface, which reduces to the Mises yield surface when anisotropy vanishes, is given by:

$$F(T_{23} - T_{33})^2 + G(T_{33} - T_{11})^2 + H(T_{11} - T_{22})^2 + 2LT_{23}^2 + 2MT_{31}^2 + 2NT_{12}^2 = 1; (13)$$

where T_{ij} represent the stress components; the subscripts 1, 2, and 3 represent the three mutually orthogonal planes of symmetry, where the direction 1 corresponds to the IDD (Figure 4); and the constants F , G , H , L , M , and N represent the square of the inverse of the yield strength under the appropriate normal and shear loading conditions. The Hill criterion requires identical yield points in tension and compression, which is generally not the case for materials exhibiting a Bauschinger effect and/or pressure dependent yield — including polymers. This criterion was applied to the PET and PVC experiments discussed above. The symmetry of the pre-orienting process, where the principal stretch ratios were as given earlier: $\lambda_1 = \lambda$, $\lambda_2 = \lambda_3 = 1/\sqrt{\lambda}$, results in the equivalence of the Hill coefficients G and H for this case. Due to the loading in these experiments, values for L and M are not required. Constants for the three remaining Hill coefficients F , G , and N were obtained from the data of the 0°, 45°, and 90° IDD tests. The resulting curves were found to predict the tensile yield at all IDDs very well. These investigators noted that oriented PET and PVC behave differently in tension and compression, exhibiting a Bauschinger effect as well as pressure dependent yield. These effects are not accounted for in the Hill Criterion. Therefore, both Rider and Hargreaves, and Brown, *et al.* modified the criterion to include a scalar internal stress, or back stress, b , which lumps the Bauschinger and pressure effects together. The modified criterion then reads as follows:

$$H(T_{11} - b - T_{22})^2 + F(T_{23} - T_{33})^2 + G(T_{33} - T_{11} + b)^2 + 2NT_{12}^2 + 2LT_{23}^2 + 2MT_{31}^2 = 1. (14)$$

Brown, *et al.* also conducted tests in simple shear on their material. The modified criterion was found to give good agreement with the shear data as well as the tensile data. We note that the material constants F , G , N and b are for a given initial draw ratio, as well as at a given strain rate and temperature. Once these material constants

have been evaluated for the desired IDR, yield can be predicted for a multiaxial state of stress for a material with that initial texture. If one is relying on this criterion to predict the yield behavior as a function of the initial texture in the material, a matrix of the material parameters F, G, H, L, M, N , and b must be assembled by conducting numerous experiments at many IDRs. Furthermore, these coefficients are valid only for cases of pre-stretches in ratio $\lambda : \frac{1}{\sqrt{\lambda}} : \frac{1}{\sqrt{\lambda}}$. We also note that this criterion is only valid for the onset of yield because it does not include effects of continuing deformation on the yield parameters, i.e., it does not furnish a formalism for the evolution of the Hill coefficients with deformation. Below, we discuss the prediction of tensile yield and flow of oriented glassy polymers with the constitutive model of this paper. An important simplifying result is that the model is based on material properties obtained from a set of experiments on the material in the isotropic state alone.

3.1.2 Constitutive Model Results

Here, we examine the plane strain tensile yield of an oriented glassy polymer² where the initial texture was obtained, for example, *via* a plane strain extrusion process, such that the texture may be described by the principal stretch ratios: $\lambda_1 = \lambda$, $\lambda_2 = 1/\lambda$, and $\lambda_3 = 1$, where λ is the IDR. We choose to consider plane strain conditions in the analyses in order to maintain a two-dimensional problem. This will be important in the later simulation of shear localization, where, had we chosen to model the tensile testing of thin specimens, the problem would become three-dimensional once localization occurs. The effects that the amount of texture and the orientation of the texture have on the initial flow response of the material are inferred by considering material samples containing various principal stretch ratios and simulating their loading at a number of different IDRs. The samples of material are assumed to have been given enough time

²For illustrative purposes, the material constants obtained for the isotropic PMMA material of Boyce, *et al.* [1987a] are used in the numerical simulations of this paper. Analyses are conducted at room temperature, where we recognize that, in reality, unoriented PMMA generally does not shear yield at this temperature, but crazes, and fractures prematurely.

to have aged after their initial processing and prior to their tensile testing. This means that any softening that occurred during the processing which produced the textured material has been negated (see Boyce, *et al.* [1987a]). This is reflected in the model by using an appropriate initial condition on the athermal shear resistance. Here, we assume the material to be fully aged, so the value for s_0 of the initially isotropic material is used. Therefore, the material again softens. The orientation and texture effects are examined by comparing the stress state at which the material begins to flow at a fixed temperature and strain rate.

For the case of plane strain tension, we compare the peak flow stress prior to softening for the IDRs of $\lambda = 1.0, 1.5, 2.0, 2.25$, and 2.5 , where the locking stretch of the material is $\lambda_L = 3.0$, over an orientation range of $\theta = 0^\circ$ to $\theta = 90^\circ$ and at a constant tensile strain rate of 0.01 sec^{-1} and a constant temperature of 25°C . Before continuing, we note here that homogeneous deformation does not actually occur in these materials after yielding because of the large tendency for deformation to localize. This is discussed in the next section. We conduct this analysis in order to obtain the values of stress at which plastic flow begins, at a given strain rate and temperature, as a function of IDR and IDD. The results are shown in Figure 6. The impact of orientation is found to increase greatly as we approach initial textures near the locking regime, *i.e.* at stretch ratios greater than 2.0 . This, of course, is due to the dramatic increase in the back stress as the locking stretch is approached. We also note that these computed curves pass through the isotropic "yield" point at an orientation θ less than 45° . By examining the flow condition for plane strain tension at a fixed strain rate and temperature and neglecting pressure effects ($\alpha = 0$), we see that the back stress acts to decrease the flow stress for values of θ less than 45° . With the further approximation $\mathbf{F}^* \doteq 1$, we obtain τ to be $[\frac{1}{2}(\mathbf{T}^* - \mathbf{B}) \cdot (\mathbf{T}^* - \mathbf{B})]^{1/2}$, where:

$$\mathbf{T} = \begin{bmatrix} 0 & 0 & 0 \\ 0 & \sigma & 0 \\ 0 & 0 & \frac{\sigma}{2} \end{bmatrix}; \quad (15)$$

and

$$\mathbf{B} = \begin{bmatrix} \cos\theta & \sin\theta & 0 \\ -\sin\theta & \cos\theta & 0 \\ 0 & 0 & 1 \end{bmatrix} \begin{bmatrix} b_1 & 0 & 0 \\ 0 & b_2 & 0 \\ 0 & 0 & b_3 \end{bmatrix} \begin{bmatrix} \cos\theta & -\sin\theta & 0 \\ \sin\theta & \cos\theta & 0 \\ 0 & 0 & 1 \end{bmatrix}; \quad (16)$$

where b_i are the principal back stress components, and the directions 1, 2, 3 and the angle θ were shown in Figure 4. The flow condition is:

$$\tau = s \left[1 - \frac{\Theta}{As} \ln \frac{\dot{\gamma}_0}{\dot{\gamma}^p} \right]^{\frac{1}{2}}, \quad (17)$$

which is constant for a given strain rate and temperature. The athermal shear strength, s , is taken to be s_0 . Incorporating equations (15) and (16) into (8) gives:

$$\frac{1}{2} \sigma^2 + \sigma (b_1 - b_2) (\sin^2 \theta - \cos^2 \theta) + b_1^2 + b_2^2 + b_3^2 = 2\tau^2. \quad (18)$$

For the case of $\theta = 45^\circ$, the tensile flow stress is $\sigma = 2\sqrt{\tau^2 - \frac{1}{2}(b_1^2 + b_2^2 + b_3^2)}$. Therefore, at an IDD of 45° , the flow stress will be less than the isotropic stress, which is given by $\sigma = 2\tau$. This decrease in flow stress is accentuated with IDR as shown in Figure 6. The results for the larger stretch ratios compare well with the trends found in the experiments discussed earlier and shown in Figure 5.

The constitutive model can be used to examine plastic flow given any general multi-axial loading condition. Yield loci can easily be obtained for any initial orientation at any fixed strain rate and temperature. The material model includes the effects of strain rate, temperature, pressure, and, of course, the additional hardening that occurs with continuing plastic deformation. Therefore, boundary value problems containing very general and inhomogeneous loading conditions may be analyzed. This is done below by investigating the effect of orientation on shear banding in glassy polymers.

3.2 Localized Flow

Many different types of materials are known to experience shear localization during plastic flow. The occurrence of this phenomenon in ductile metals, single crystals, and geological materials has been reviewed by Rice [1976]. Shear localization is a

phenomenon which is of great interest because it affects such a broad spectrum of materials and can have a marked impact on all subsequent deformation in the material, often leading to fracture. Solutions determining the conditions necessary for the onset of shear localization in various isotropic material models have been obtained for the rate-independent case (Rudnicki and Rice [1975], Rice [1976]) and the rate-dependent case (Anand, *et al.* [1987]). Finite element analysis may also be used to predict the direction of shear banding after artificially initiating localization with either a material or geometric imperfection (Tvergaard, *et al.* [1981], Needleman and Tvergaard [1984]).

3.2.1 Localization in Pre-Oriented Polymers

Experiments on pre-oriented polymers have shown that shear localization is affected by both the degree and orientation of the initial texture in the material. This effect has been examined experimentally by Duckett [1975] and Brown and Ward [1968] in the fully oriented semi-crystalline (nearly amorphous) polymer PET below its Θ_s ; by Duckett, *et al.* [1972] in the highly oriented semi-crystalline polymer PP above its Θ_s ; and by Rider and Hargreaves [1969] in the amorphous polymer PVC. In these experiments, textured polymers were tested at various IDDs (and various IDRs for the PVC case) in simple tension. The resulting shear band direction (SBD) was recorded. This direction is given by the angle ψ shown in Figure 4. The experiments on the semi-crystalline polymer sheets showed the SBD to be closer to the tensile axis than the IDD except for IDDs of $\theta \leq 16^\circ$, in which cases shear banding was difficult to observe, *i.e.* homogeneous deformation was obtained. Rider and Hargreaves' plots of the SBD as a function of IDD of PVC at various draw ratios are shown in Figure 7. The data is from tensile tests on thin sheets which have been oriented such that the principal stretch ratios are given by: $\lambda_1 = \lambda$, $\lambda_2 = \lambda_3 = 1/\sqrt{\lambda}$. This experimental data indicate that the SBD depends on the specific material, the initial draw ratio, and the orientation. As the IDR increases, its impact on the direction of shear localization

becomes stronger, especially as the locking stretch ratio is neared. This shows that the SBD, ψ , is dependent on both material and IDR, i.e., the effect of IDR on the material response is relative to the locking stretch of the specific material. We can see these effects in the amorphous PVC data where the IDR has a very large impact on the SBD as a function of orientation, θ . Figure 7 shows that at a low IDR, the SBD is not significantly impacted by the orientation θ of the IDD, and the ψ of the SBD becomes a strong function of θ as the IDR increases and approaches the effective locking stretch of the material.

These investigators (Duckett [1975], Brown and Ward [1968], Duckett, *et al.* [1972]) have been able to analytically predict the direction of shear banding in these polymers with reasonable accuracy by using Hill's anisotropic theory of yield (equation 5) and a normality (associated) flow rule. The resulting analysis predicts two directions for the formation of a shear band. These predicted directions agreed well with the experimental data and were further improved upon by using the Hill criterion as modified with a scalar back stress, which was described earlier. We emphasize that using this method requires experimentally obtaining the Hill coefficients and the scalar back stress at each draw ratio.

Once the material has localized and a prominent shear band forms, the material within the band reorients toward the tensile axis. This phenomenon has been experimentally observed in PET (Brown and Ward [1968]), PP (Duckett, *et al.* [1972]), and PVC (Rider and Hargreaves [1970]) by examining the deformed material with a polarizing microscope. The extinction direction corresponds to the maximum refractive index which is parallel to the (local) principal stretch direction. The extinction direction in the band was found to be different from that of the bulk material. The extinction direction within the band rotated from the IDD towards the tensile axis by an angle ($\theta - \bar{\theta}$), where $\bar{\theta}$ is the angle that the principal stretch ratio within the band currently makes with the tensile axis. This data indicated that the material within the band reorients towards the loading axis. Brown and Ward had additional results

showing that the greater the amount of applied tensile deformation, the greater the amount of reorientation. This was more clearly demonstrated by Rider and Hargreaves in their results on PVC, which are shown in the plots of Figure 8. These plots show the orientation, θ , of the material within the band with respect to the tensile axis as a function of the applied nominal stretch ratio. The nominal stretch is determined from the total applied displacement and the initial gage length. We note that the local stretch in the shear band would be much greater due to the localization of the deformation in the region. The initial orientation at unit stretch is the angle of the IDR. These results indicate that the material within the band continues to reorient as it is stretched until the orientation direction is parallel with the tensile axis. Rider and Hargreaves' results also demonstrate that the reorientation occurs faster, i.e. at lower nominal stretch ratios, when the IDR is smaller. This, of course, is due to the fact that there is less re-orienting to accomplish. Our analysis below will examine the phenomenon of reorientation within the shear band.

3.2.2 Numerical Simulation of Localization

The case of a plane strain tensile test of oriented PMMA at room temperature was analyzed here using the constitutive model of Boyce, *et al.* [1987a] with appropriate initial values for A^i and s . A point of principal interest was the effect of material orientation on the direction of shear banding in glassy polymers. A relatively coarse mesh of 4-node plane strain elements (ABAQUS type CPE4) was used in the finite element analysis. This element is the constant dilation 4-node element of Nagtegaal, *et al.* [1974], where the shear and pressure terms are integrated separately to prevent "locking" of the mesh. We note that a sharper shear band could be picked up with a finer mesh and/or a mesh of quadrilateral elements composed of constant strain triangle (CST) elements (Needleman and Tvergaard [1984]). The element size defines the minimum possible thickness of the band. Therefore, an analysis with a finer mesh

of 4-node elements could result in a narrower shear band. The shear band will form along element boundaries. The CST mesh formation provides a greater freedom for the deformation to localize because of the larger number and direction of element boundaries. Also, because these are constant strain elements, large strains can occur in an element without necessarily affecting its neighboring elements. This, of course, is precisely the physical response of shear banding. If one is interested in obtaining a narrow band, and the direction of the band is known *a priori*, then one could tailor a CST mesh to accurately pick up the localized straining. However, the purpose of this analysis was to compute the direction of the shear banding. Therefore, the coarse unbiased mesh of quadrilateral elements shown in Figure 8 was chosen, although it may result in an artificially broad shear band.

The simulation to be discussed is for the plane strain tensile testing of a pre-oriented glassy polymer, where the plane of straining during the pre-orienting process and the subsequent testing are identical. The problem becomes asymmetric with respect to the tensile axis when the principal direction of orientation is aligned at some angle with respect to the tensile axis. The asymmetry of the problem which results from material pre-orientation permits a model of one-half of the test specimen to be used with appropriate boundary conditions. This condition is enforced by constraining the nodes on the bottom of the mesh on either side of the specimen center to displace in equal and opposite *x* and *y* directions. Due to the material orientation, shear band formation in the central portion of the specimen may result in rotation of the specimen. This was permitted to occur by constraining the nodes along the top of the mesh to remain on a straight line, but by giving them the freedom to contract as well as pivot about the center node of this surface. This is equivalent to loading the specimen in a pinned grip. The center node of the bottom surface of the mesh is constrained in the *x*- and *y*-directions. The center node of the top surface of the mesh is constrained in the *x*-direction only and is displaced in the *y*-direction to the desired extension. The half-length of the specimen was chosen to be four times the width in order to allow the

shear band to grow unhindered along a straight path until reaching a free surface.

The shear band is initiated in the center of the specimen by making the two bottom center elements of the mesh softer than the remainder of the mesh. This was done by assigning these elements a lower value for the material property of the athermal shear resistance, $s_0 = 105 \text{ MPa}$, than the rest of the elements of the mesh, which were assigned $s_0 = 112 \text{ MPa}$. This caused a shear band to emanate from this point once the material began to flow. Different perturbation values of $s_0 < 112 \text{ MPa}$ were tried on these two elements in a test case to ascertain its effect on the resulting shear band direction. It was found to have no effect.

The analysis was conducted on a mathematical model with the same material constants as determined by Boyce, *et al.* [1987a] for PMMA. The material was taken to be oriented to varying levels of texture such that the principal values of the initial textures were given by: $\lambda_1 = \lambda$, $\lambda_2 = 1/\lambda$, $\lambda_3 = 1$, where λ is the initial draw ratio, and λ_3 coincides with the plane strain direction of the simulation. The material was then "tested" in plane strain tension at the initial draw ratios of $\lambda = 2.0$, 2.25 , and 2.50 , and the initial draw directions of $\theta = 0^\circ$, 30° , 45° , 60° , and 90° . The direction of shear banding was obtained by examining contours of the plastic strain rate where regions of intense plastic straining indicate the development of a shear band. The angle that these regions make with the tensile axis gives the direction of banding. Two bands of concentrated straining initially form in each sample. These bands are at approximately 90° to one another with possibly a few degrees difference (Anand and Spitzig [1982]) due to the pressure dependent yield of the polymer which is included in the constitutive model. The angle, ψ , at which the shear band formed with respect to the tensile axis is depicted in Figure 10, where it is shown to change with both initial draw ratio and direction. These numerical results demonstrate that as the IDR approaches the locking regime, where the locking stretch of PMMA is $\lambda_L = 3.0$, the dependence of the shear band direction on orientation becomes more acute. This follows the trends found in experiments discussed earlier, which showed that the more highly textured

the polymer, the greater is the dependence of shear band direction on orientation.

Another interesting result of the numerical analysis is illustrated in Figure 11. This figure shows the contours of plastic strain rate as deformation progresses for the cases where the IDR is initially oriented with the tensile axis. For the high draw ratio of 2.5, we see that the material at first begins to localize into symmetric 45° shear bands; however, the straining soon becomes uniform throughout the test specimen. This was also observed in the experiments on highly oriented semi-crystalline PET where clearly defined shear bands were not observed at orientations of $\theta < 15^\circ$. Duckett, *et al.* did not comment on any test they may have conducted at 0° orientation on polypropylene. Rider and Hargreaves did not obtain distinct banding for $\lambda = 2.0$ and $\theta = 0^\circ$ or for $\lambda = 3.3$ and $\theta = 0^\circ, 15^\circ$ in their PVC samples. It appears that they did not test the highest draw ratio at these orientations for this reason.

The absence of shear banding in these experimental cases as well as the numerical simulations at 0° orientation can be explained by analogy with a Considére stability analysis. In the isotropic material, necking occurs in the Considére construction at the point when the slope of the stress-strain curve equals the stress, σ , divided by the stretch, λ , or $\frac{d\sigma}{d\lambda} = \frac{\sigma}{\lambda}$. Stability is regained and cold-drawing begins at a second Considére point. The highly preoriented material which is aligned with the tensile axis is essentially at a state past the second Considére point and in the middle of a stable cold-drawing mode, which even the artificial initiation of localization cannot supersede. Referring to the stress-stretch curve for isotropic PMMA, our material of IDR=2.5 was past this second Considére point whereas the lower IDR of 2.25 was before but quite near this point. Therefore, we can expect the material with IDR=2.5 to continue in the stable drawing mode and the material with IDR=2.25 to require a greater amount of applied strain before localization disappears and stable cold-drawing takes over. This is exactly what was predicted with the model as illustrated in Figure 11, which demonstrates that a larger applied stretch was needed before homogeneous drawing occurred in the material with an IDR of 2.25 than in the material with an IDR of 2.5.

Our model correctly predicts this continued drawing.

It is also of interest to observe the development of a shear band in those cases where the IDR is aligned asymmetrically about the tensile axis. The case of an IDR of $\lambda=2.5$ and an IDD of $\theta= 30^\circ$ was chosen to examine this development. Figures 12 and 13 depict the contour plots of plastic shear strain rate and plots of the deformed mesh as deformation progresses for this case. For purposes of illustration, the asymmetry conditions were used to depict both halves of the specimen. The plots of the deforming mesh show the deformation to be concentrated in a shear band. The material asymmetry also causes a slight shearing of the bulk of the specimen. The plastic shear strain rate contours illustrate the increase in intensity, with deformation, of straining within the band, where the plastic shear strain rate is as much as five times greater than the applied nominal tensile strain rate of 0.01sec^{-1} . The rate contours for the case of $\theta = 30^\circ$ also show the broadening of the band where the region of highest shear strain rate moves away from the center of the specimen. This indicates that the material near the specimen center, where the shear band initially formed, is now essentially "locked". Therefore, active plastic deformation spreads up (and down) the specimen, thus, broadening the band. We also observe two concentrated bands of intense straining in the initial stages of deformation. However, as deformation progresses, one band disappears, and we eventually form a single distinct shear band through the first and third quadrants of the specimen, which also contains the IDD. This is in agreement with experimental observations. However, the second band which appeared in the initial stages of our numerical analysis is, on occasion, the shear band which forms in the experiments. We note that direct comparisons between our plane strain numerical results and the experimental results on thin tensile specimens cannot be made due to the different constraints of these tests, where thinning of the bands is permitted in the experiments.

We were also able to predict the reorientation of the material within the band. The amount of reorientation was found to depend on the applied deformation. Figure 14

depicts the computed reorientation of the material within the band for the case of an IDR of 2.5 and an IDD of 30° as a function of the applied stretch. We note here that the applied stretch (nominal) is relative to the total specimen length of 8.0 units, whereas the active plastic deformation occurs over a gauge length of approximately 2.6 units. We see the material reorients toward the tensile axis by a greater amount as the applied tensile stretch increases. These results are in accord with those found in the experiments discussed earlier.

4 Concluding Remarks

In this paper, the effect of preorientation on the inelastic deformation behavior of glassy polymers was examined. This effect was incorporated into the constitutive model of Boyce, Parks, and Argon [1987a] via the use of appropriate initial conditions on internal state variables. This method of modelling texture in a material takes full advantage of the concept of internal state variables. The model was subsequently used in conjunction with the finite element method to analyze the homogeneous and localized flow of oriented glassy polymers. Comparing the results of our numerical simulations to trends found in similar experiments, we found that our model correctly assesses the initial flow behavior, as well as several complicated responses resulting from the inhomogeneous process of shear localization. These include the direction of shear banding as a function of initial orientation conditions, material reorientation within the band, and the conditions which result in continued cold drawing of the specimen. The numerical analyses did not require any further experimental material property identification beyond the isotropic material properties and the initial texture.

We have shown that the model in its current form is capable of successfully capturing many of the major effects of initial texture on inelastic deformation in glassy polymers. However, in order to obtain a complete constitutive description, many items still need to be addressed. One such item, important for both initially isotropic and oriented

polymers, is the effect of the physical aging process on plastic flow. Temperature and strain rate have also been observed to affect the strain hardening response of glassy polymers (Hope, *et al.* [1980], Botto, *et al.* [1987]). This effect is considered to be the result of a relaxation of the network structure (Raha and Bowden [1972], Kahar, *et al.* [1978], Boyce [1986], Botto, *et al.* [1987]). Additionally, extreme terminal hardening has been observed in crystallizable polymers such as PET, whose initial structure was amorphous (Ward [1984]). This degree of hardening cannot be entirely explained by the backstress of the current formulation and could be of major importance in the response of highly oriented polymers. These features, which require further experimental quantification and modelling, are currently under investigation.

Acknowledgements

The authors gratefully acknowledge the support of NSF under Grant #8405995-MEA and DARPA under contract #N00014-86-K-0768. We also wish to acknowledge the donation of the DG MV10000 computer from the Data General Corporation. The ABAQUS finite element code was made available under academic license from Hibbit, Karlson, and Sorensen, Inc., Providence, RI.

References

1950 Hill, R., **The Mathematical Theory of Plasticity**, Oxford University Press, Oxford.

1968 Brown, N., Ward, I.M., "Deformation Bands in Oriented PET", *Phil. Mag.*, 17, p.961.

1968 Haward, R.N. and G. Thackray, "The Use of a Mathematical Model to Describe Isothermal Stress-Strain Curves in Glassy Thermoplastics", *Proc. Roy. Soc. 302*, p.453.

1969 Brown, N., Duckett, R.A., Ward, I.M., "The Yield Behavior of Oriented PET", *Phil. Mag.*, 18, p.483.

1969 Lee, E.H., "Elastic-Plastic Deformation at Finite Strains", *ASME Jnl. Appl. Mech.* 56, p.1.

1969 Rider, J.G., Hargreaves, E., "Yielding of Oriented PVC", *J. Poly. Sci., A-2*, 7, p.829.

1970 Kramer, E.J., "Stress Aging in Anhydrous Nylon 6-10", *Jnl. Appl. Phys.* 41, p.4327.

1970 Rider, J.G., Hargreaves, E., "Optical Anisotropy in Oriented PVC", *J. Phys. D: App. Phys.*, 3, p.993.

1971 Rawson, F.F., Rider, J.G., "Effects of Internal Stress on the Yielding of Oriented PVC", *J. Poly. Sci., C*, 33, p.87.

1971 Wright, H., Faraday, C.S.N., White, E.F.T., and Treloar, L.R.G., "The elastic constants of oriented glassy polymers", *J. Phys. D*, 4, p.2002.

1972 Duckett, R.A., Goswami, B.C., Ward, I.M., "Molecular Reorientation in PP", *J. Poly. Sci., Phys. Ed.*, 10, p.2167.

1972 Raha, S. and P.D. Bowden, "Birefringence of Plastically Deformed PMMA", *Polymer* 13, p.174.

1973 Argon, A.S., "A Theory for the Low-Temperature Plastic Deformation of Glassy Polymers", *Phil. Mag.* 28, p.39.

1973 Bahadur, S., "Strain Hardening Equation and the Prediction of Tensile Strength of Rolled Polymers", *Poly. Eng. Sci.*, 19, p.266.

1974 Nagtegaal, J.C., Parks, D.M., Rice, J.R., "On Numerically Accurate Finite Element Solutions in the Fully Plastic Range", *Comp. Meth. Appl. Mech. Eng.* 4, p.153.

1975 Duckett, R.A., "Anisotropic Yield Behavior", Ch. 11 of **Structure and Properties of Oriented Polymers**, ed. Ward, I.M., App. Sci. Pub. Ltd., London.

1975 Hadley, D.W., "Small Strain Elastic Properties", Ch. 9 of **Structure and Properties of Oriented Polymers**, ed. Ward, I.M., App. Sci. Pub. Ltd., London.

1975 Kocks, U.F., Argon, A.S., and M.F. Ashby, "Thermodynamics and Kinetics of Slip", **Progress in Materials Science** 19, Pergamon, Oxford.

1975 Rice, J.R., "Continuum Mechanics and Thermodynamics of Plasticity in Relation to Microscale Deformation Mechanisms", in **Constitutive Equations in Plasticity**, ed. A.S. Argon, MIT Press, Cambridge, MA.

1975 Rudnicki, J.W., Rice, J.R., "Conditions for the Localization of Deformation in Pressure-Sensitive Dilatant Materials", *J. Mech. Phys. Solids*, 23, p.371.

1976 Rice, J.R., "The Localization of Plastic Deformation", **Proceedings of the 14th International Congress of Theoretical and Applied Mechanics**, Vol. I, p.207, North-Holland, Amsterdam.

1978 Kahar, N., Duckett, R.A. and I.M. Ward, "Stress Optical Studies of Oriented PMMA", *Polymer* 19, p.136.

1978 Struik, L.C.E., **Physical Aging in Amorphous Polymers and Other Materials**, Elsevier, Amsterdam.

1980 Haward, R.N., "The Effect of Chain Structure on the Annealing and Deformation Behavior of Polymers", *Coll. and Poly. Sci.* 258, p.42.

1980 Hope, P.S., Ward, I.M., and A.G. Gibson, "The Hydrostatic Extrusion of PMMA", *Jnl. Mat. Sci.* 15, p.2207.

1981 Tvergaard, V., Needleman, A., Lo, K.K., "Flow Localization in the Plane Strain Tensile Test", *J. Mech. Phys. Solids*, 29, p.115.

1982 Anand, L., Spitzig, W.A., "Shear-Band Orientation in Plane Strain", *Acta Met.*, 30, p.553.

1982 Onat, E.T., "Representation of Inelastic Behavior in the Presence of Anisotropy and Finite Deformations", in **Recent Advances in Creep and Fracture of Engineering Materials and Structures**, eds. B. Wilshire and D.R.J. Owen, Pineridge Press, Swansea.

1983 Loret, B., "On the Effects of Plastic Rotation in the Finite Deformation of Anisotropic Elastoplastic Materials", *Mech. of Matls.*, p.287.

1983 Nemat-Nasser, S., "On Finite Plastic Flow of Crystalline Solids and Geomaterials", *Jnl. Appl. Mech.* 50, p.1114.

1984 ABAQUS, version 4.5, Hibbit, Karlsson, and Sorensen, Inc., Providence, RI.

1984 Needleman, A., Tvergaard, V., "Finite Element Analysis of Localization in Plasticity", Chap. 3 in **Finite Elements, Special Problems in Solid Mechanics** V, ed. Oden, J.T., Carey, G.F., Prentice Hall, Englewood Cliffs, NJ.

1984 Parks, D.M., Argon, A.S., and B. Bagepalli, "Large Elastic-Plastic Deformation of Glassy Polymers", MIT Program in Polymer Science and Technology Report, MIT, Cambridge, MA.

1984 Ward, I.M., "The Role of Molecular Networks and Thermally Activated Processes in the Deformation Behavior of Polymers", *Poly. Eng. Sci.*, 24, p.724.

1985 Anand, L., "Constitutive Equations for Hot-Working of Metals", *Int. Jnl. of Plasticity* 1, p. 213.

1985 Argon, A.S., Megusar, J., Grant, N.J., "Shear Band Induced Dilations in Metallic Glasses", *Scripta Met* 19, p.591.

1985 Dafalias, Y.F., "The Plastic Spin", *ASME Jnl. Appl. Mech.*, p. 865.

1986 Boyce, M.C., "Large Inelastic Deformation of Glassy Polymers", PhD Thesis, Dept. of Mechanical Engineering, MIT.

1987 Anand, L., Kim, K.H., Shawki, T.G., "Onset of Shear Localization in Viscoplastic Solids", *J. Mech. Phys. Solids* 35, p.407.

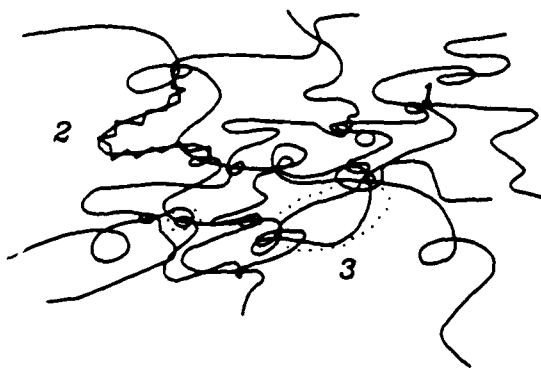
1987 Botto, P.A., Duckett, R.A., and I.M. Ward, "The Yield and Thermoelastic Properties of Oriented PMMA", *Polymer* 28, p.257.

1987 Boyce, M.C., Parks, D.M., Argon, A.S., "Large Inelastic Deformation of Glassy Polymers, Part I: Rate-Dependent Constitutive Model", to appear in *Mech. of Materials*.

1987 Boyce, M.C., Parks, D.M., Argon, A.S., "Large Inelastic Deformation of Glassy Polymers, Part II: Numerical Simulation of Hydrostatic Extrusion", to appear in *Mech. of Materials*.

1987 Boyce, M.C., Parks, D.M., Weber, G.G., "On the Kinematics of Finite Strain Plasticity", in preparation.

1987 Onat, E.T., "Representation of Elastic-Plastic Behavior in the Presence of Finite Deformations and Anisotropy", submitted to *Int. Jnl. Plasticity*.



1. physical entanglement
2. N rigid links between entanglements
3. intermolecular interaction

Figure 1. Schematic of amorphous polymer.

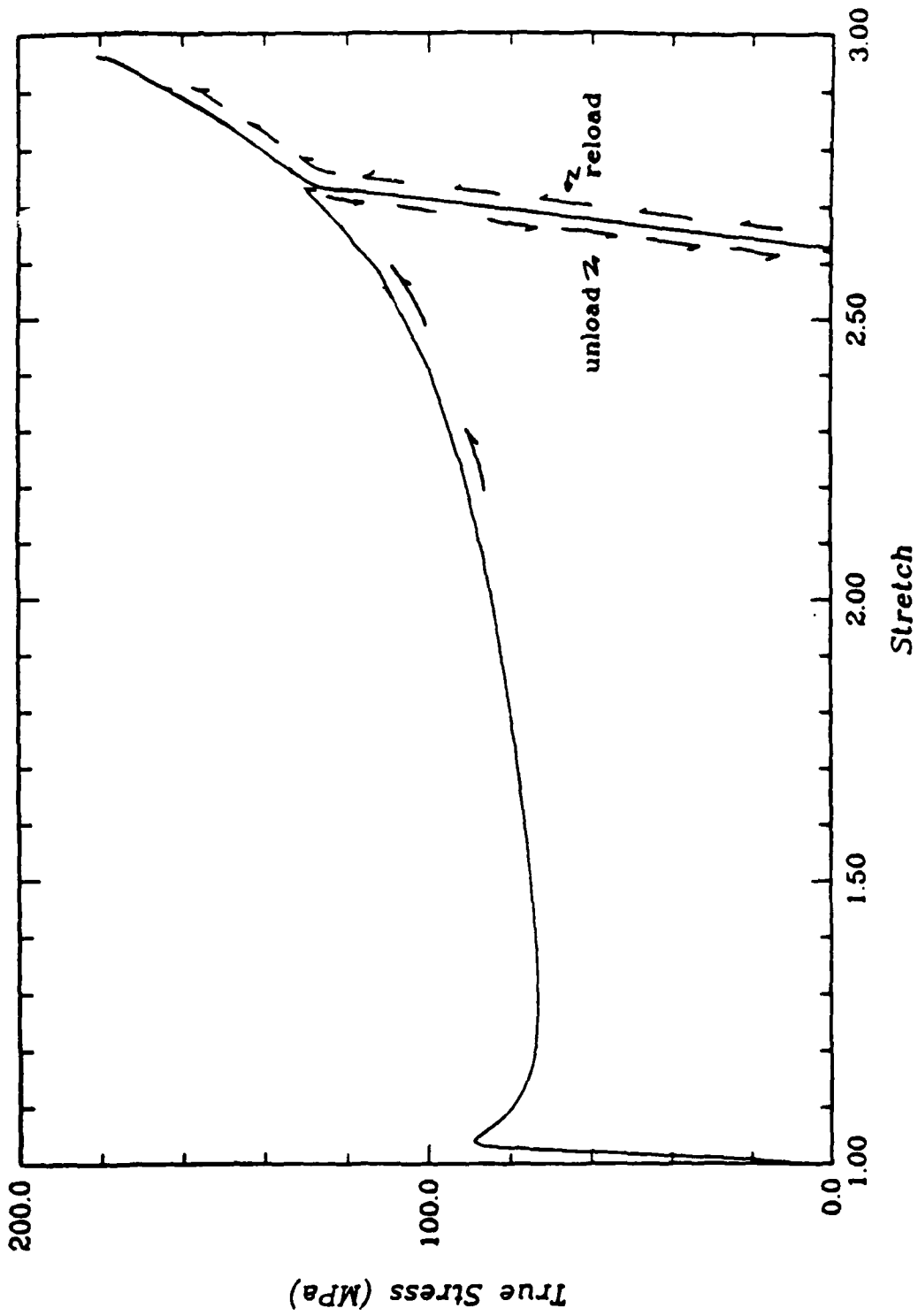


Figure 2. Tensile true stress-stretch curve for PMMA at $\dot{\epsilon} = 0.01 \text{ sec}^{-1}$ and $\Theta = 25^\circ\text{C}$ showing loading, unloading, and reloading.

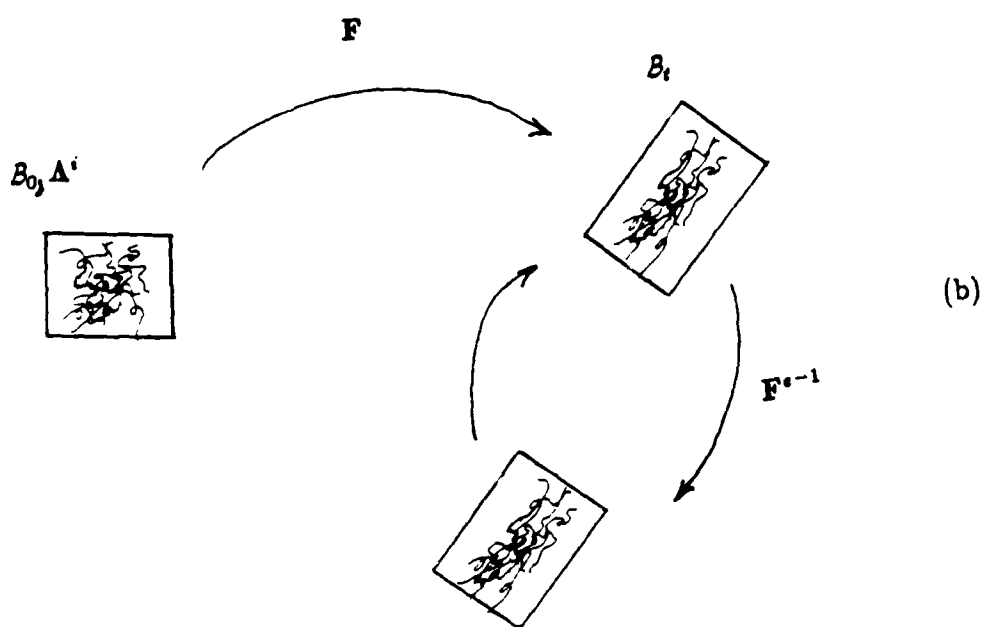
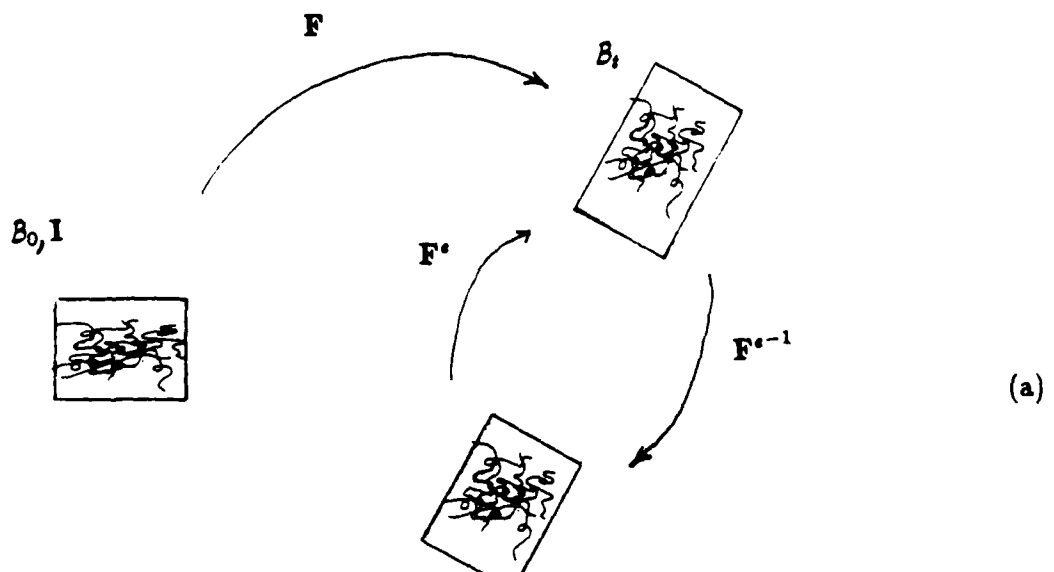


Figure 3. (a) Deformation of an initially isotropic body; (b) Deformation of a pre-oriented (textured) body, where the initial texture is described by A^i .

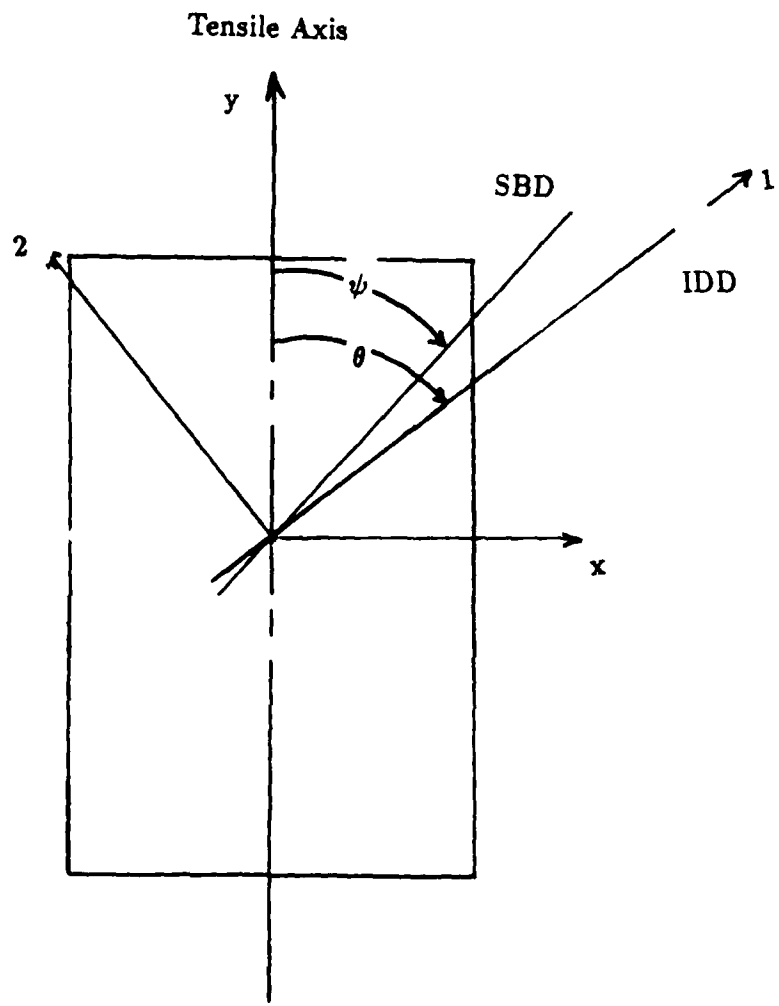


Figure 4. Schematic of a pre-textured tensile specimen. The angle between the tensile axis and the initial draw direction (IDD) is given by θ . The angle between the tensile axis and the shear band (SBD) is given by ψ .

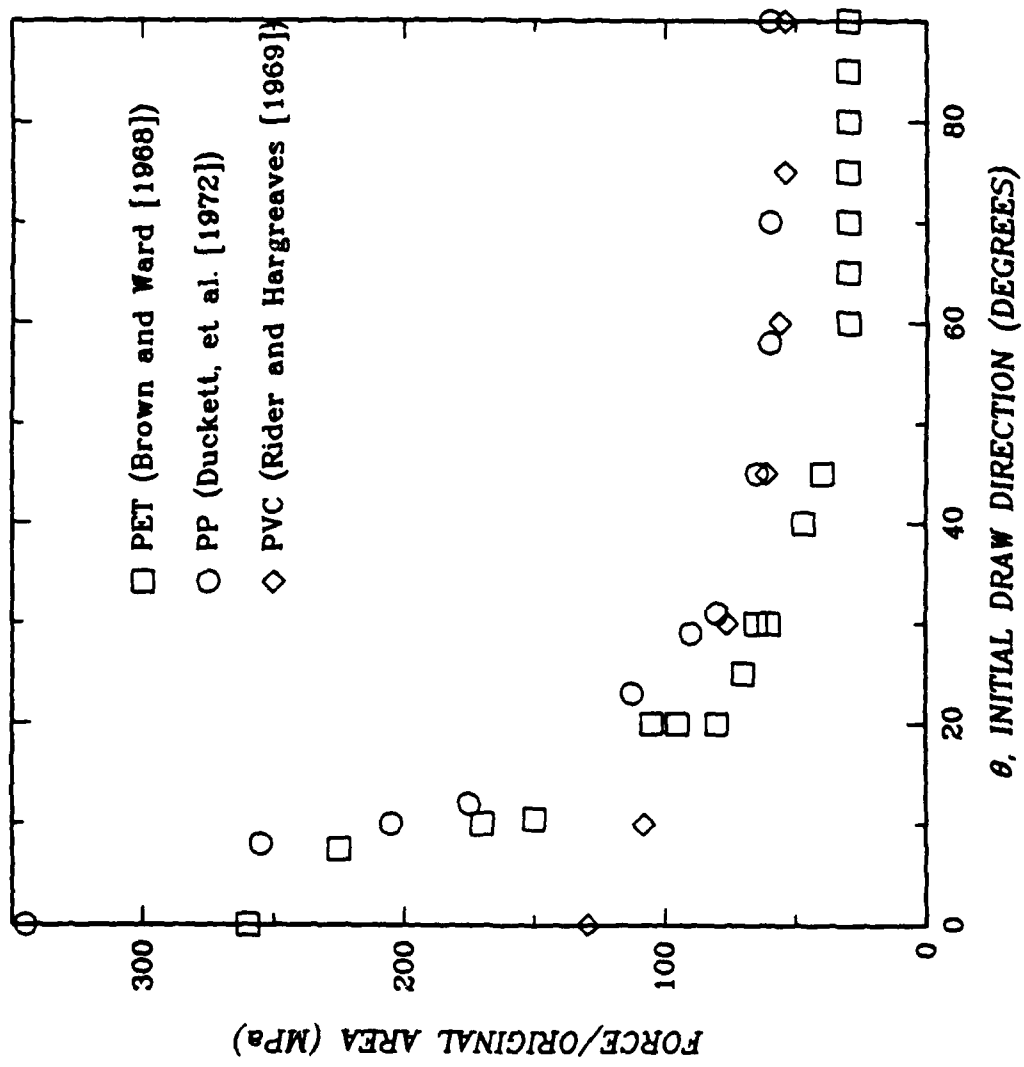


Figure 5. Nominal tensile yield stress as a function of θ , initial draw direction, for highly oriented PET and PP, and for PVC of IDR=3.3.

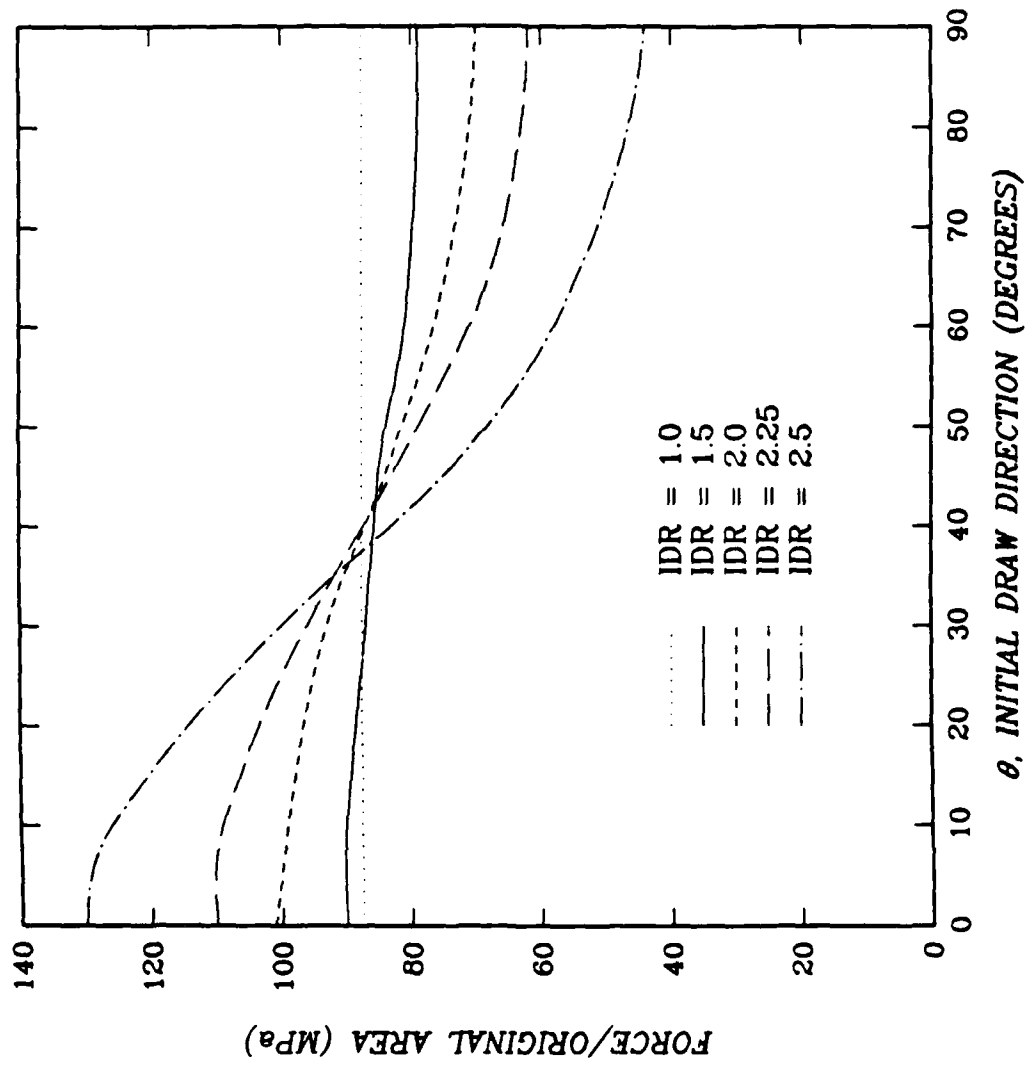


Figure 6. Computed peak flow stress as a function of θ , initial draw direction, for various initial draw ratios (IDR) for PMMA at $\Theta = 25^\circ\text{C}$.

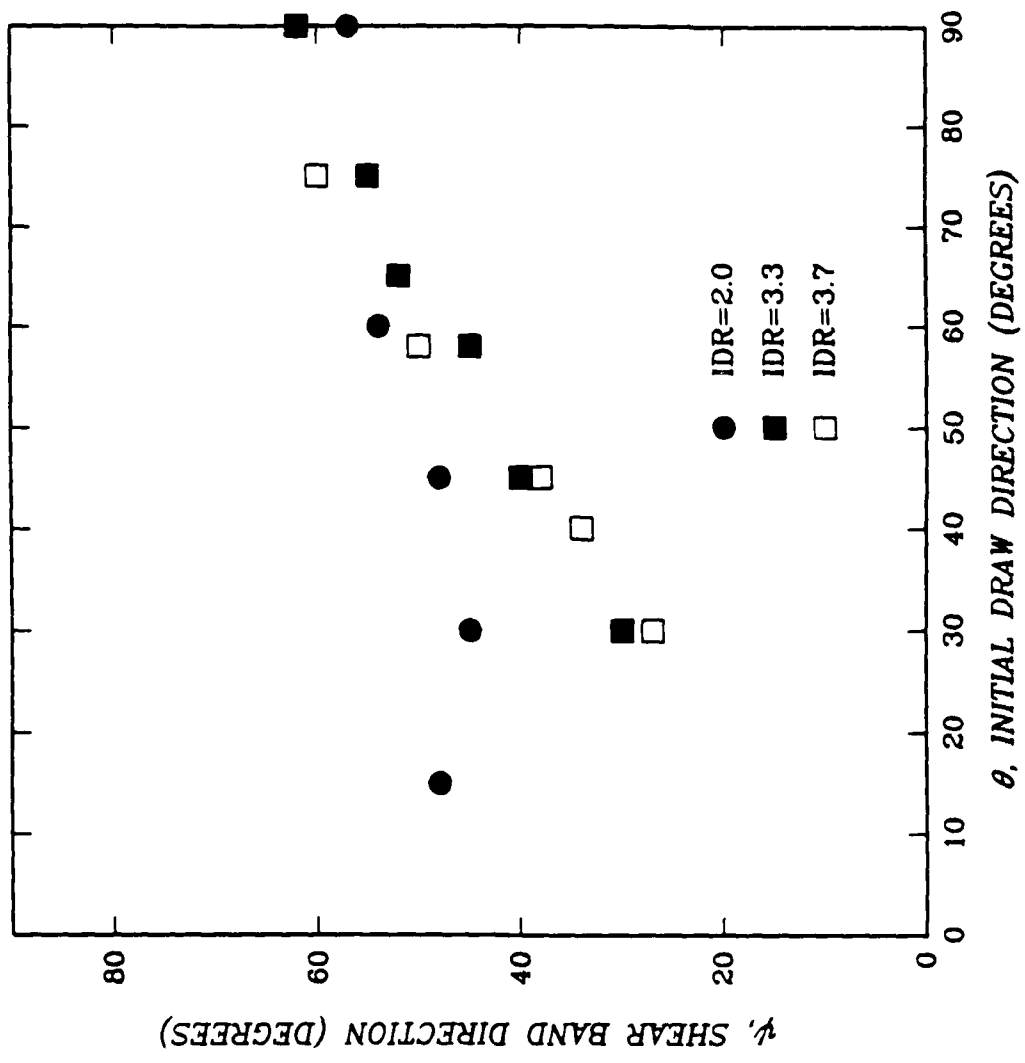


Figure 7. Rider/Hargreaves experimental results for shear band direction, ψ , as a function of initial draw direction, θ , for various draw ratios in amorphous PVC.

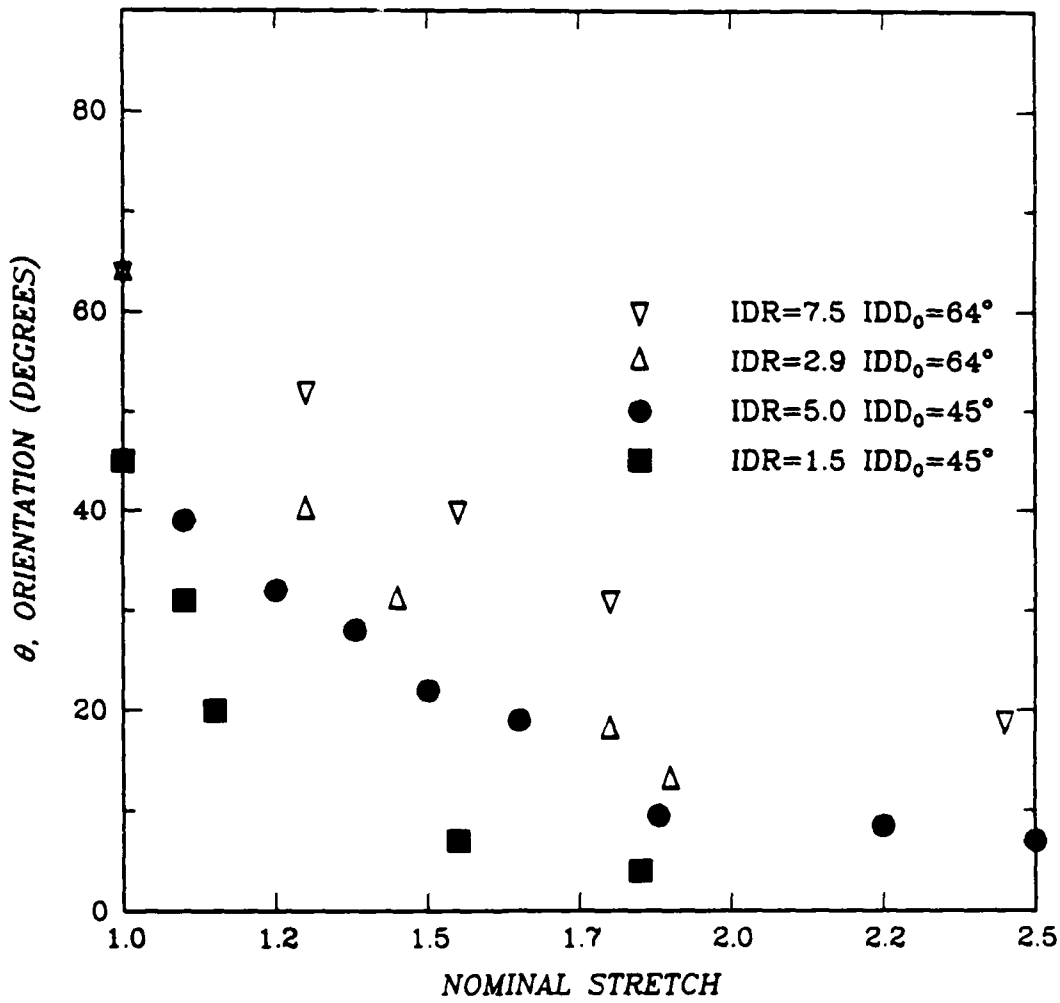


Figure 8. Rider/Hargreaves experimental results on amorphous PVC for material orientation, θ , within shear band as a function of nominal stretch for IDR of 5.0 and 1.5 given and IDD of 45°, and IDR of 7.5 and 2.9 given an IDD of 64°.

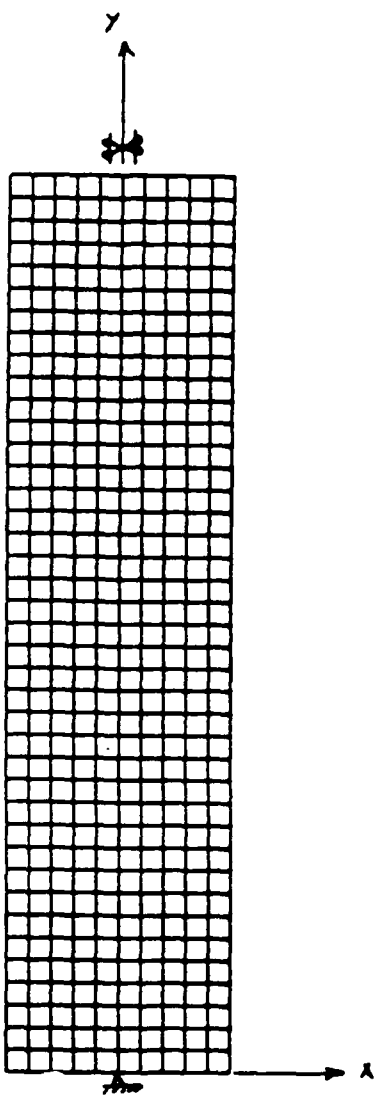


Figure 9. Finite element model of one-half of a plane strain tensile test specimen. Boundary conditions consist of constraining nodes on either side of the specimen center along the bottom surface of the mesh to displace in equal and opposite x- and y-directions. The nodes along the top surface are constrained to remain on a straight line. The top center node is constrained in the x-direction.

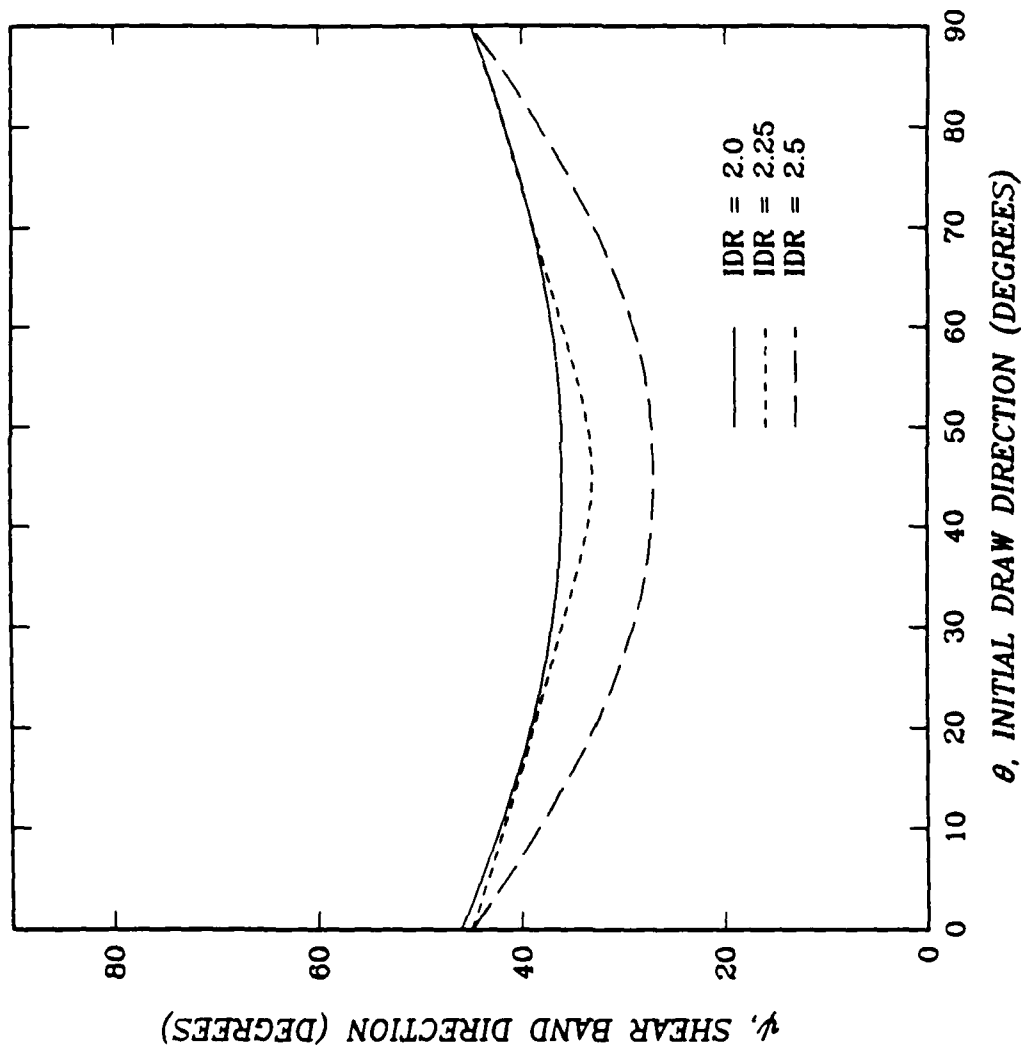


Figure 10. Shear band direction, ψ , as a function of initial draw direction, θ , for various initial draw ratios in PMMA. These results were computed from simulated plane strain tensile tests.

Values of $\dot{\gamma}^p$ (sec $^{-1}$)

- 1) 0.0
- 2) 0.0021
- 3) 0.0042
- 4) 0.0063
- 5) 0.0084
- 6) 0.0105
- 7) 0.0126
- 8) 0.0147
- 9) 0.0168

IDR = 2.5

IDD, $\theta = 0^\circ$

$\lambda_{flow} = 1.035$



$\lambda = 1.05$



$\lambda = 1.06$

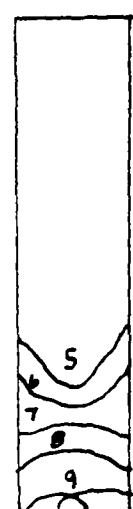
IDR = 2.25

IDD, $\theta = 0^\circ$

$\lambda_{flow} = 1.042$



$\lambda \approx 1.05$



$\lambda = 1.085$

Figure 11. Contours of plastic shear strain rate for an IDD of 0° and IDRs of 2.25 and 2.5 for PMMA at different applied stretches. Note that homogeneous deformation (cold drawing of sample) is obtained at a lower stretch ratio for the higher IDR. λ_{flow} is the applied nominal stretch at which flow begins.

Values of $\dot{\gamma}^p$ (sec $^{-1}$)

- 1) 0.0
- 2) 0.0073
- 3) 0.0145
- 4) 0.0218
- 5) 0.0290
- 6) 0.0363
- 7) 0.0436
- 8) 0.0509
- 9) 0.0581
- 10) 0.0654

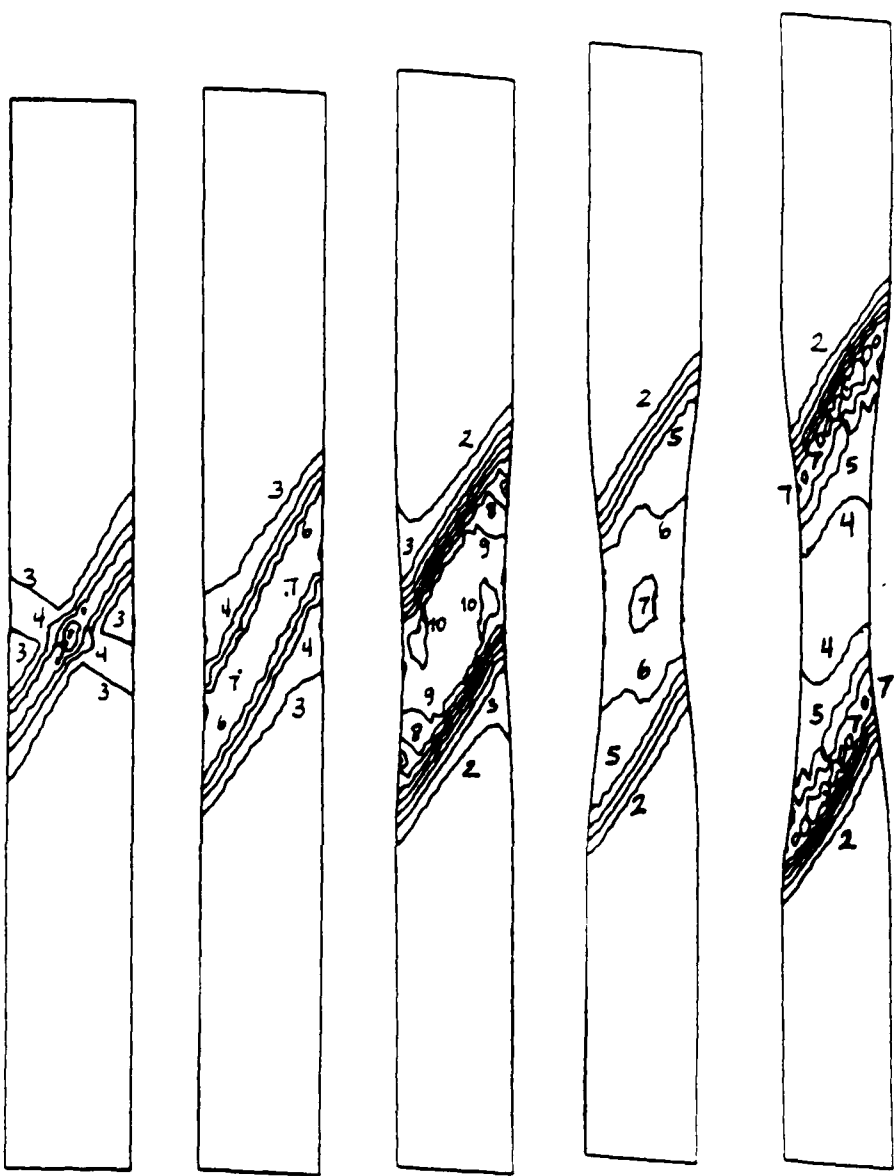


Figure 12. Contour plots of plastic shear strain rate as a function of deformation for the case of an IDR of 2.5 and an IDD of 30°.

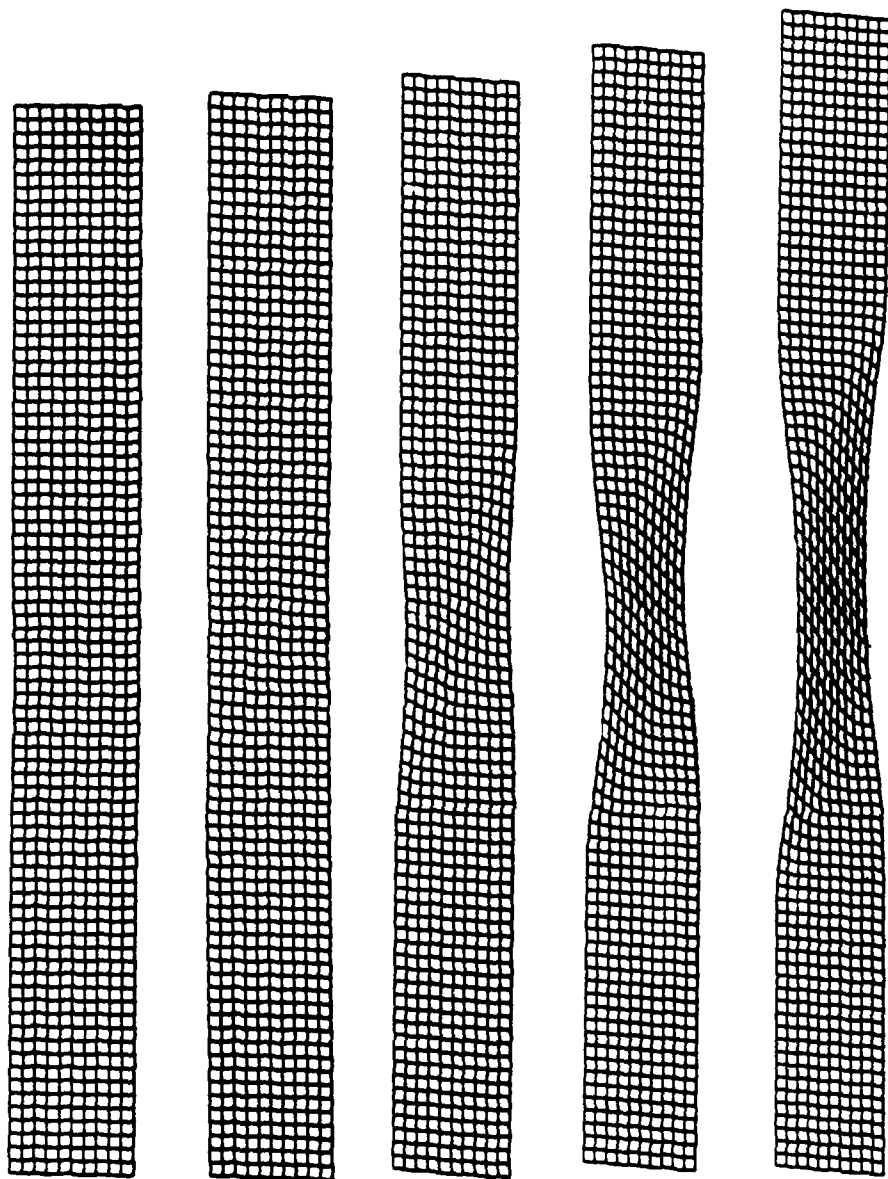


Figure 13. Plots of the mesh as deformation progresses, clearly illustrating the development of a shear band for the case of an IDR of 2.5 and an IDD of 30°.

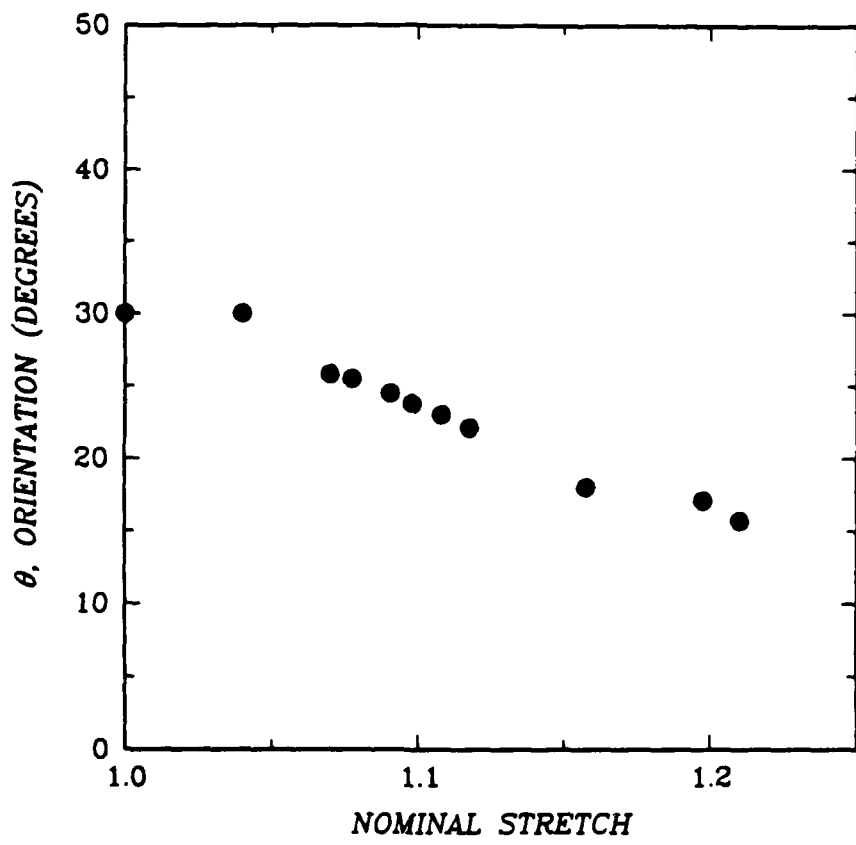


Figure 14. Numerical results for material orientation, θ , within the shear band as a function of nominal stretch for an IDR of 2.5 and IDD of 30° for PMMA.